microbial biotechnology

Safety of photosynthetic *Synechococcus elongatus* for *in vivo* cyanobacteria–mammalian symbiotic therapeutics

Kiah M. Williams,[1] (iD) Hanjay Wang,[1] Michael J. Paulsen,[1] Akshara D. Thakore,[1] Mary Rieck,[2] Haley J. Lucian,[1] Frederick Grady,[1] Camille E. Hironaka,[1] Athena J. Chien,[1] Justin M. Farry,[1] Hye Sook Shin,[1] Kevin J. Jaatinen,[1] Anahita Eskandari,[1] Lyndsay M. Stapleton,[1,3] Amanda N. Steele,[1,3] Jeffrey E. Cohen[1] and Y. Joseph Woo[1,3,*]

[1]*Department of Cardiothoracic Surgery, Stanford University, 300 Pasteur Drive, Falk Cardiovascular Research Building, Stanford, CA 94305, USA.*
[2]*Beckman Center for Molecular and Genetic Medicine, Stanford University, Stanford, CA, USA.*
[3]*Department of Bioengineering, Stanford University, Stanford, CA, USA.*

Summary

The cyanobacterium *Synechococcus elongatus* (SE) has been shown to rescue ischaemic heart muscle after myocardial infarction by photosynthetic oxygen production. Here, we investigated SE toxicity and hypothesized that systemic SE exposure does not elicit a significant immune response in rats. Wistar rats intravenously received SE ($n = 12$), sterile saline ($n = 12$) or *E. coli* lipopolysaccharide (LPS, $n = 4$), and a subset (8 SE, 8 saline) received a repeat injection 4 weeks later. At baseline, 4 h, 24 h, 48 h, 8 days and 4 weeks after injection, clinical assessments, blood cultures, blood counts, lymphocyte phenotypes, liver function tests, proinflammatory cytokines and immunoglobulins were assessed. Across all metrics, SE rats responded comparably to saline controls, displaying no clinically significant immune response. As expected, LPS rats exhibited severe immunological responses. Systemic SE administration does not induce sepsis or toxicity in rats, thereby supporting

the safety of cyanobacteria–mammalian symbiotic therapeutics using this organism.

Introduction

Oxygen is the second most abundant gas in Earth's atmosphere (Cavendish, 1785) and is essential for the maintenance and healing of all tissues in the human body. Indeed, hypoxia plays a central role in myocardial infarction, cerebral ischaemia, diabetic microvascular disease, the healing of skin ulcers and many other disease states (Darby and Hewitson, 2016). Although numerous drugs and revascularization strategies have been developed to treat these diseases, none function mechanistically by directly producing oxygen for the tissue at risk. Thus, oxygen-producing biomaterials are increasingly being investigated (Gholipourmalekabadi *et al.*, 2016), and photosynthetic cyanobacteria in particular have the potential to alleviate a diverse array of medical maladies by directly delivering oxygen to hypoxic tissues (Wang *et al.*, 2019).

Cyanobacteria are a phylum of photosynthetic prokaryotic organisms that occupy fresh, brackish and marine waters around the world. Using sunlight to convert carbon dioxide and water into oxygen and glucose, cyanobacteria are among the primary producers of environmental oxygen (Hamilton *et al.*, 2016). Previously, our team described a novel photosynthetic symbiotic therapy to rescue ischaemic myocardium, utilizing the cyanobacterium *Synechococcus elongatus* to take up cardiomyocyte-derived carbon dioxide and release new oxygen for sustained aerobic metabolism during ischaemia (Cohen *et al.*, 2017). Treatment with *S. elongatus* in rodent hearts produced a 25-fold increase in tissue oxygen levels, enhanced cellular metabolism and increased cardiac output by nearly 60% relative to ischaemic controls. Although our initial study included a preliminary safety assessment and demonstrated no obvious immune response by rats against *S. elongatus*, a comprehensive *in vivo* acute and chronic immunologic analysis is required before our novel therapy can be translated to the clinical setting.

Some species of cyanobacteria have been linked to illness in humans and other animals after oral ingestion or skin exposure. Reported complications have included flu-like symptoms, gastroenteritis, skin rashes and in rare

cases liver failure due to hepatotoxin exposure during cyanobacterial blooms (Jochimsen *et al.*, 1998; Stewart *et al.*, 2006). The majority of epidemiological studies about cyanobacterial exposure, however, report no significant findings, and some have demonstrated that various cyanobacteria are seemingly harmless to animals after ingestion or direct injection into tissue (Alvarez *et al.*, 2015; Chávez *et al.*, 2016; Cohen *et al.*, 2017). Moreover, it is believed that illness from cyanobacteria exposure is due to ingestion of large amounts of cyanotoxins that have accumulated in water during blooms, rather than an ability of the organism to invade and colonize a host (Codd *et al.*, 2005). *S. elongatus*, our organism of interest, has a fully sequenced genome, does not produce any known toxins and has not been linked to any cases of morbidity or mortality when introduced into animals *in vivo*, but the details of its immunogenicity and safety have not been previously evaluated.

To thoroughly investigate the safety of our novel cyanobacterial therapy, we performed serial intravenous injections of *S. elongatus*, sterile saline or *E. coli* lipopolysaccharide (LPS) in rats (Fig. 1). LPS, also known as endotoxin, is a powerful antigen that is found on Gram-negative bacteria such as *E. coli*. It is comprised of Lipid A, O Antigen and core oligosaccharide, and can lead to sepsis through uncontrolled activation of the TLR4 signalling pathway (Beutler, 2000; Alexander and Rietschel, 2001; Heumann and Roger, 2002; Kaya *et al.*, 2005; Martin *et al.*, 2015). At baseline and multiple time points after each injection with *S. elongatus*, saline or LPS, clinical assessments, blood cultures, blood counts, lymphocyte phenotypes, liver function tests, proinflammatory cytokines and immunoglobulins were assessed. We hypothesized that systemic *in vivo* exposure to *S. elongatus* does not produce any clinically significant distress, inflammation or immune activation in rats.

Results

S. elongatus *does not produce clinical distress or septic syndrome*

After single and serial tail vein injection of either saline or 2.5×10^8 cells of *S. elongatus*, all rats retained their usual activities, socialization, grooming behaviours, appetite and tissue perfusion. Conversely, rats that received intravenous LPS became pale and cool to the touch on their ears and tails, antisocial, anorexic and poorly groomed within one day of injection. LPS rats also had significant lacrimation, mucus membrane bleeding and lethargy (Table 1).

Time-course changes in rectal temperature and body weight are shown in Fig. S1. At all time points studied, rats that received *S. elongatus* maintained normal body temperatures, similar to those that received saline. At 24 h after the first injection, saline rats had a temperature of 36.5 ± 0.17 °C compared with 36.6 ± 0.23 °C for *S. elongatus* rats ($P = 0.99$), where the normal body temperature of rats ranges from 35.9 to 37.5 °C (Ades, 2019). Rats receiving LPS, however, became febrile after 24 h (37.5 ± 0.28 °C, $P = 0.049$ vs. saline). Additionally, while saline and *S. elongatus* rats retained comparable percentages of their original body weight, LPS rats exhibited significant weight loss at 24 h
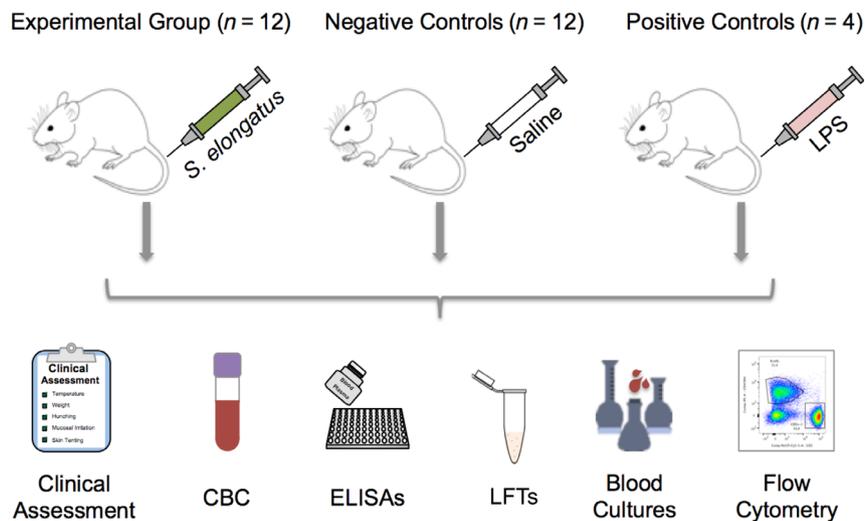
Fig. 1. Methodology overview. Rats were injected with either *S. elongatus*, sterile saline or LPS, and monitored according to the depicted metrics over the course of 4 weeks. After 4 weeks, a subset of animals in the experimental *S. elongatus* group (*n* = 8) and negative control saline group (*n* = 8) received an additional identical injection and were similarly assessed for another 4 weeks before necropsy. CBC, complete blood count; ELISA, enzyme-linked immunosorbent assay; LFTs, liver function tests; LPS, lipopolysaccharide.

Table 1. Clinical assessment findings. Clinical assessment results for each rat in the three treatment groups, showing severe signs of distress in rats that received LPS and mild signs for those injected with saline or *S. elongatus*. Assessment occurred immediately before each blood draw and was blinded between saline and *S. elongatus* rats.

Saline			*S. elongatus*			LPS		
ID	Inj.	Signs of distress	ID	Inj.	Signs of distress	ID	Inj.	Signs of distress
S1	1	None	C1	1	None	L1	1	Poorly groomed, lacrimation, fur raised, hunching, lethargy, poor socialization, anorexic, blood on nose
	2	None		2	None			
S2	1	None	C2	1	None			
	2	Poor grooming		2	None			
S3	1	None	C3	1	None			
	2	Hypervocalization		2	Left eye proptosis	L2	1	Lacrimation, squinting, fur raised, poor socialization, anorexic, poor grooming, hunching, lethargy, blood on nose
S4	1	Anorexic	C4	1	None			
	2	Ulcer on shoulder		2	None			
S5	1	None	C5	1	None			
	2	None		2	None			
S6	1	None	C6	1	Anorexic	L3	1	Tail cold to touch, lacrimation, fur raised, hunching, anorexic, lethargy, blood on nose, poor socialization
	2	None		2	None			
S7	1	None	C7	1	Anorexic			
	2	None		2	None			
S8	1	None	C8	1	Hypervocalization			
	2	None		2	None	L4	1	Squinting, lacrimation, fur raised, hunching, anorexic, lethargy, dragging back legs, blood on nose, low socialization
S9	1	None	C9	1	None			
S10	1	None	C10	1	None			
S11	1	None	C11	1	None			
S12	1	None	C12	1	Loose stool			

ID, animal identification code; Inj., injection number; LPS, lipopolysaccharide.

$(95.3 \pm 0.89\%$ vs. $98.7 \pm 0.52\%$ for saline, $P = 0.037$) and at 48 h post-injection $(93.4 \pm 0.40\%$ vs. $98.3 \pm 0.77\%$ for saline, $P = 0.0001$). By 8 days after injection, saline and *S. elongatus* rats had exceeded their original body mass $(103.0 \pm 1.7\%$ and $102.0 \pm 1.3\%$, respectively, $P = 0.83$), but LPS rats were still only $96.9 \pm 1.6\%$ of their baseline weight $(P = 0.057$ vs. saline).

Rats do not mount a significant acute immune response to *S. elongatus*

Data regarding complete blood count (CBC) findings at 24 h after injection are presented in Table 2. By 24 h post-injection, the number and distribution of white blood cells (WBCs) were similar between the rats that received saline and those that received *S. elongatus*. Conversely, the rats that received LPS exhibited significant neutrophilia ($P = 0.0010$), and complementary lymphopaenia ($P = 0.0015$) after 24 h compared with saline controls. Rats that received *S. elongatus* were mildly thrombocytopaenic ($P = 0.0081$) at 24 h after injection, while rats that received LPS were severely thrombocytopaenic ($P < 0.0001$) compared with saline controls.

In fact, CBC derangements were observed within 4 h of LPS injection, including significant leukopaenia (4560 ± 550 vs. 8350 ± 920 cells μl^{-1} at baseline, $P = 0.020$), neutrophilia ($61.3 \pm 2.3\%$ vs. $17.5 \pm 3.2\%$ of WBCs at baseline, $P = 0.014$) and lymphocytopaenia ($36.0 \pm 2.2\%$ vs. $74.3 \pm 3.1\%$ of WBCs at baseline, $P = 0.016$; Figs S2 and S3). Although rats that received saline or *S. elongatus* also exhibited a neutrophilic shift

Table 2. Complete blood count (CBC) results 24 h after injection. Values of complete blood count (CBC) components 24 h after the first injection, displaying only mild thrombocytopaenia in *S. elongatus* rats but profound thrombocytopaenia, neutrophilia and lymphopaenia in LPS rats. Baseline values represent the mean $\pm$ SEM across all groups prior to the first injection.

CBC findings	Baseline values	Saline	*S. elongatus*	LPS
Platelet count (platelets μl^{-1})	913 000 $\pm$ 29 000	869 000 $\pm$ 29 000	728 000 $\pm$ 33 000**	328 000 $\pm$ 33 000****
White blood cell count (cells μl^{-1})	9130 $\pm$ 490	11 000 $\pm$ 870	11 300 $\pm$ 880	10 600 $\pm$ 1000
Neutrophil (%)	15.0 $\pm$ 1.1	18.1 $\pm$ 1.3	20.8 $\pm$ 2.8	73.3 $\pm$ 4.5**
Lymphocyte (%)	77.7 $\pm$ 1.3	77.3 $\pm$ 1.4	75.1 $\pm$ 2.9	24.5 $\pm$ 4.8**
Monocyte (%)	5.93 $\pm$ 0.52	3.70 $\pm$ 0.73	3.80 $\pm$ 0.73	2.00 $\pm$ 0.41
Eosinophil (%)	1.33 $\pm$ 0.23	0.917 $\pm$ 0.29	0.417 $\pm$ 0.19	0.250 $\pm$ 0.25

LPS, lipopolysaccharide.
*. Significant vs. saline ($P < 0.05$), **significant vs. saline ($P < 0.01$), ***significant vs. saline ($P < 0.001$), ****significant vs. saline ($P < 0.0001$).

following injection, their response was far less profound and occurred more gradually than that observed in LPS rats, with no significant neutrophil increase from baseline until 48 h after injection (saline: $30.5 \pm 2.8\%$ vs. $13.2 \pm 1.4\%$ of WBC at baseline, $P = 0.0011$; *S. elongatus*: $29.5 \pm 2.6\%$ vs. $16.2 \pm 1.7\%$ of WBCs at baseline, $P = 0.0062$). For both the saline and *S. elongatus* groups, neutrophil percentages normalized within 8 days of injection. At every time point, the neutrophil percentage and all other WBC changes in *S. elongatus* rats were comparable to those observed in rats that received only saline. Eosinophil, basophil and monocyte percentages were comparable between all groups at all times, and absolute cell counts of all WBC subtypes largely reflected the same trends (Fig. S4).

Flow cytometric analysis with gating of lymphocyte subpopulations (Fig. 2A–I) revealed non-significant differences between all groups at all times, with the following exceptions: significantly more $CD3^+$ T-cells in LPS rats compared with saline rats at baseline ($40.1 \pm 0.93\%$ vs. $32.7 \pm 2.2\%$ of lymphocytes, $P = 0.014$); significantly fewer $CD4^+$ T cells as a percentage of $CD3^+$ T cells in LPS rats compared with saline rats 4 h after the first injection ($65.3 \pm 3.3\%$ vs. $79.3 \pm 3.9\%$, $P = 0.048$); significantly fewer activated $CD4^+$ T cells in *S. elongatus* rats compared with saline rats 4 h after the first injection ($3.49 \pm 0.40\%$ vs. $5.51 \pm 0.44\%$ of $CD4^+$ T cells, $P = 0.0080$); significantly fewer activated $CD8^+$ T cells in LPS rats compared with saline rats 8 days after the first injection ($0.370 \pm 0.11\%$ vs. $1.02 \pm 0.24\%$ of $CD8^+$ T cells, $P = 0.048$); and a decreased percentage of B cells in LPS rats compared with saline rats 4 h after the first injection ($17.2 \pm 1.8\%$ vs. $31.4 \pm 2.0\%$, $P = 0.0016$) (Fig. 2J).

Proinflammatory cytokine levels were measured 4 h after the initial injection (Fig. 3). None of the cytokine levels were statistically significantly different between rats that received *S. elongatus* and those that received saline, although there was an apparent difference in TNF-α levels, which were elevated in rats that received *S. elongatus* (115 ± 43 pg ml^{-1} vs. 2.07 ± 1.4 pg ml^{-1} saline, $P = 0.067$). Rats that received LPS had elevated IL-1β (149 ± 21 pg ml^{-1} vs. 38.0 ± 18 pg ml^{-1}, $P = 0.029$), IL-6 (40.9 ± 9.2 ng ml^{-1} vs. 0.953 ± 0.72 ng ml^{-1}, $P = 0.014$), KC/GRO (33.9 ± 1.2 ng ml^{-1} vs. 0.0880 ± 0.017 ng ml^{-1}, $P < 0.0001$) and TNF-α (229 ± 35 pg ml^{-1} vs. 2.07 ± 1.4 pg ml^{-1}, $P = 0.0007$) compared with saline controls at 4 h after the first injection.

Rats do not mount a significant adaptive immune response to S. elongatus

At 4 weeks after the first injection, a subset of saline and *S. elongatus* rats ($n = 8$, each) received a repeat injection. CBC results and flow cytometric analysis following the repeat injection revealed no significant differences between the two groups. Both groups experienced a neutrophilic shift more rapidly after the second injection than after the first injection, with significant increases in neutrophils occurring within 4 h for rats that received saline ($29.5 \pm 2.6\%$ vs. $16.0 \pm 2.4\%$ at baseline, $P = 0.026$), and within 24 h for rats that received *S. elongatus* ($39.6 \pm 4.8\%$ vs. $19.5 \pm 2.1\%$ at baseline, $P = 0.045$). Lymphocyte subpopulation distributions were comparable between rats that received a second injection of saline and those that received a second injection of *S. elongatus* at all times (Fig. 2; Figs S2–S4).

Additionally, plasma IgG and IgM levels were non-significantly different between saline and *S. elongatus* rats at 8 days after the first injection and at 24 h, 48 h and 8 days after the second injection. IgM was significantly higher in *S. elongatus* rats at 4 weeks after the first injection (0.385 ± 0.038 mg ml^{-1} vs. 0.137 ± 0.029 mg ml^{-1}, $P = 0.028$; Fig. 4).

S. elongatus *does not persist in blood*

All blood cultures from the *S. elongatus* rats (taken 4 h, 24 h, 48 h, 8 days and 4 weeks post-injection) were negative for cyanobacterial growth after one week of incubation, both by microscopy of liquid media and by plating on solid media with incubation for 3 additional weeks (Fig. 5). All positive controls grown alongside the experimental samples showed *S. elongatus* growth either by observation of motile auto-fluorescent rods on fluorescence microscopy (100%, 23 of 23 examined) or by growing bright green colonies or lawns on solid media after 3 weeks (71%, 20 of 28 examined).

S. elongatus *does not induce acute or chronic liver damage*

Rats injected with saline or *S. elongatus* had similar levels of AST ($P = 0.90$), ALT ($P = 0.68$), alkaline phosphatase ($P = 0.68$) and total bilirubin ($P = 0.69$) at 24 h after the first injection. Conversely, LPS rats had mildly elevated AST ($P = 0.094$) and alkaline phosphatase ($P = 0.10$), and significantly elevated ALT ($P = 0.014$) and total bilirubin ($P = 0.0004$) compared with saline rats at that time (Table S1). Four weeks after injection, liver enzyme levels in saline and *S. elongatus* rats remained similar.

S. elongatus *does not colonize or damage tissue in rats*

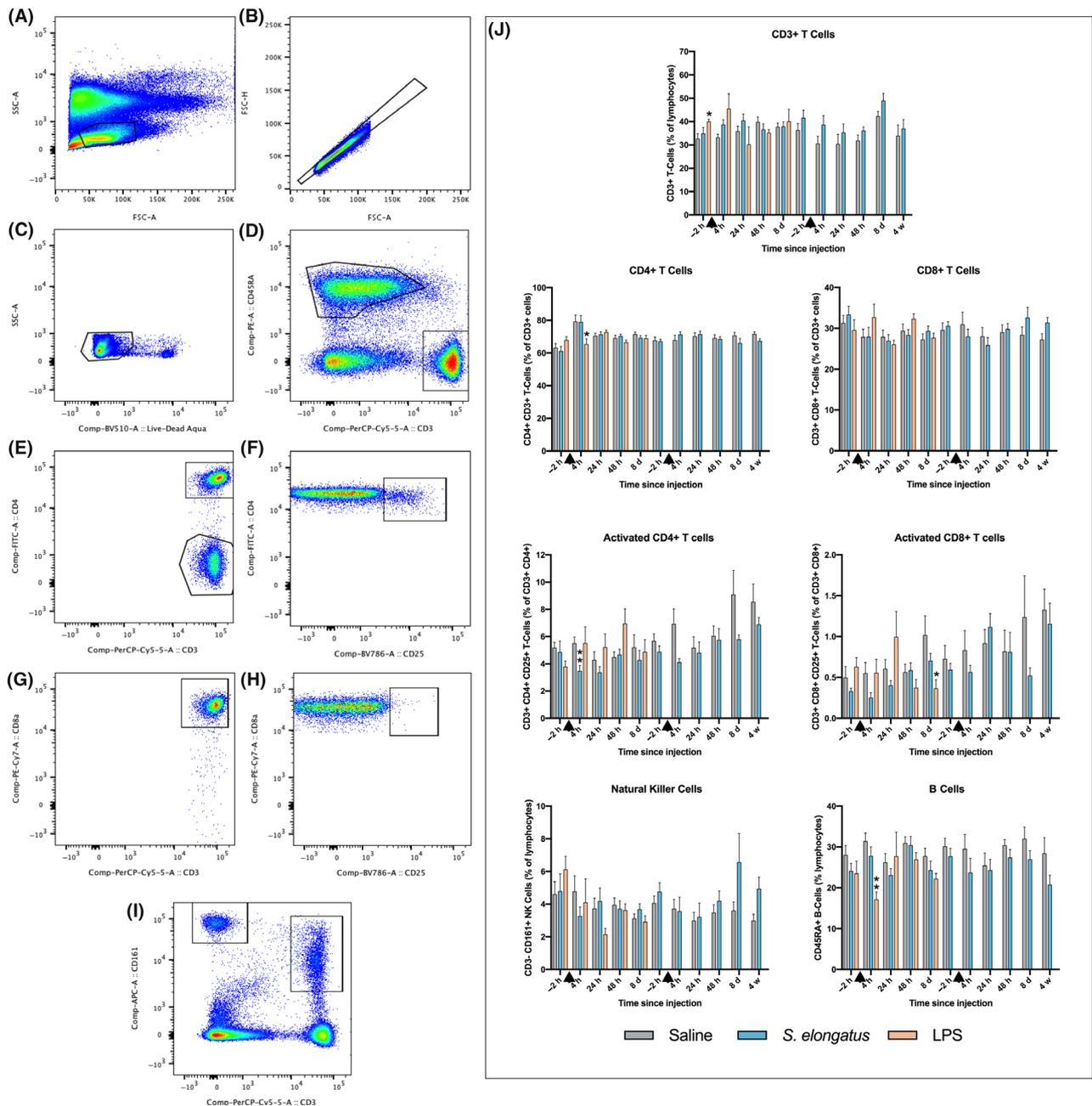Tissue histology examination by an independent veterinary pathologist who was blinded to the experimental

Fig. 2. Flow cytometry gating and lymphocyte subpopulation quantification. The gates represent the following populations: (A) Total lymphocytes, (B) single cells, (C) live cells, (D) CD45RA$^+$ B cells (upper left) and CD3$^+$ T cells (lower right), (E) CD3$^+$CD4$^+$ T cells (upper) CD3$^+$CD4$^-$ T cells (lower), (F) CD3$^+$ CD4$^+$CD25$^+$ activated T cells, (G) CD3$^+$CD8a$^+$ T cells, (H) CD3$^+$CD8a$^+$CD25$^+$ activated T cells, (I) CD3$^-$CD161$^+$ natural killer cells (left) and CD3$^+$CD161$^+$ cells (right). (J) Cytometric findings of lymphocyte subpopulations of rats injected with saline (n = 8–12), *S. elongatus* (n = 8–12) or LPS (n = 3–4). Results are presented as percentages of parent populations, and demonstrate minimal differences between rats administered saline and *S. elongatus*, with minor T- and B-cell changes for those administered LPS. Rats administered LPS were euthanized prior to the second injection. Error bars represent SEM, and black arrows indicate time of injection. d, days; h, hours; LPS, lipopolysaccharide; w, weeks. *=significant vs. saline ($P < 0.05$), **=significant vs. saline ($P < 0.01$), ***=significant vs. saline ($P < 0.001$), ****=significant vs. saline ($P < 0.0001$).

groups revealed no signs of bacterial infection or related damage to the major tissues (heart, lung, liver, spleen, kidney, adrenal gland, eyes, testes, accessory sex glands, salivary gland, pancreas, lymph node, tongue, trachea, thyroid gland, thymus, oesophagus, stomach, small intestine, large intestine, skin, cerebrum, cerebellum white and brown adipose tissue, and skull). Two *S. elongatus* rats, one saline rat and one LPS rat had
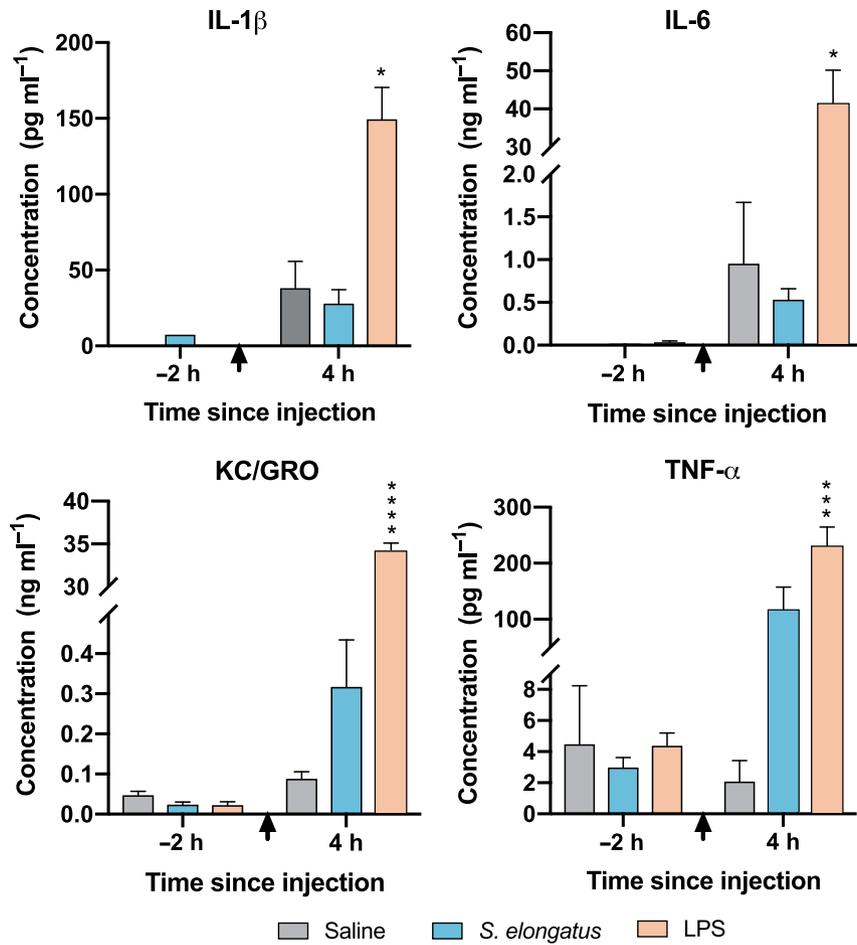
Fig. 3. Proinflammatory cytokine quantification 4 h after injection. Cytokine concentrations from peripheral blood surrounding the first injection of either saline ($n = 6$), *S. elongatus* ($n = 8$) or LPS ($n = 4$), displaying a prominent acute inflammatory response to LPS, and a detectable but not statistically significant response to *S. elongatus*. Error bars represent SEM, and black arrows indicate time of injection. Statistical analysis was performed using two-tailed unpaired Student's *t*-tests. h, hours; IL, interleukin; KC/GRO, keratinocyte chemoattractant/growth-regulated oncogene; LPS, lipopolysaccharide; TNF-α, tumour necrosis factor α. *=significant vs. saline ($P < 0.05$), **=significant vs. saline ($P < 0.01$), ***=significant vs. saline ($P < 0.001$), ****=significant vs. saline ($P < 0.0001$).
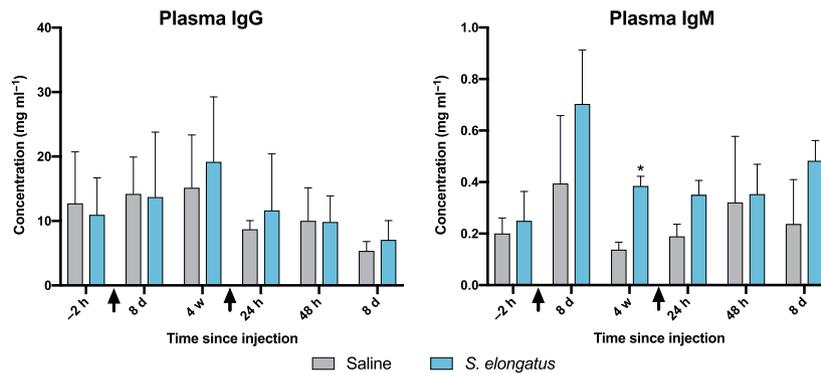

Fig. 4. Immunoglobulin concentrations surrounding both injections. Adaptive immune activity as measured by IgG and IgM immunoglobulins, surrounding two serial injections of either saline ($n = 4$) or *S. elongatus* ($n = 4$). Error bars represent SEM, and black arrows indicate time of injection. d, days; h, hours; Ig, immunoglobulin; w, weeks. *=significant vs. saline ($P < 0.05$).
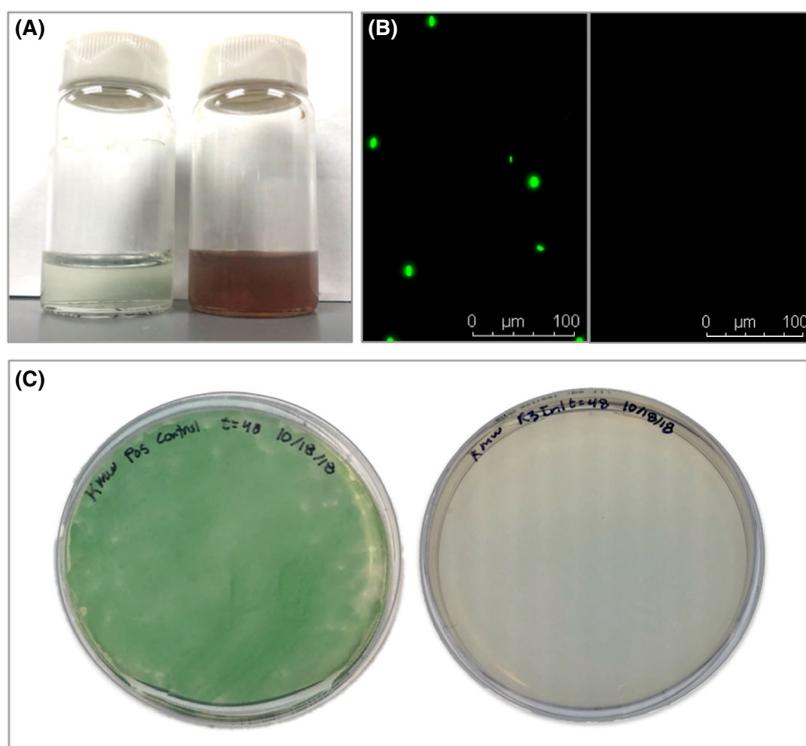
Fig. 5. Blood cultures specific to *S. elongatus*. Blood cultures for *S. elongatus* were negative, suggesting its inability to persist in rat blood after *in vivo* administration.
A. Vials of *S. elongatus* in BG11 (left) and blood from a rat injected with *S. elongatus* in BG11 (right).
B. A positive control *S. elongatus* blood culture (left) and blood from a rat injected with *S. elongatus* (right) under Texas Red.
C. Positive control *S. elongatus* plated on BG11 (left) and blood from a rat injected with *S. elongatus* plated on BG11 (right).

tissue damage behind their eyes due to repeated retro-orbital blood collection.

Discussion

Although *S. elongatus* is of great scientific interest in the context of direct bioconversion of carbon dioxide into fuels and plastic precursors (Atsumi *et al.*, 2009; Carbonell *et al.*, 2019), metabolic engineering to enhance production of fatty acids (Santos-Merino *et al.*, 2018), circadian rhythm biology (Fleming and O'Shea, 2018) and many additional applications, its interaction with mammalian immunological processes has not previously been detailed. This study comprehensively assessed the safety of intravenous administration of *S. elongatus* cyanobacteria in rats *in vivo* to inform future exploration of this organism's utility in symbiotic therapeutics. Serial systemic administration of *S. elongatus* did not result in any observable signs of infection or distress, any significant inflammatory changes in WBC subtype quantities or any statistically significant increase in proinflammatory cytokines. Additionally, *S. elongatus* did not persist in blood and did not cause appreciable organ or tissue damage. These findings

were validated by use of a positive control group of rats that received LPS from *E. coli*.

Typically, when bacteria are introduced into the bloodstream of an animal, there is a rapid activation of the complement system, causing recruitment of phagocytic neutrophils and activation of mast cells to release proinflammatory mediators (Heesterbeek *et al.*, 2018). Subsequently, the leftover bacterial antigens are presented by dendritic cells to T lymphocytes, resulting in a continued inflammatory response and development of antibodies by B lymphocytes (Alberts *et al.*, 2002, Karim and Fadi, 2015). The latter process leads to adaptive immunity to an antigen and allows for rapid immune reactivation upon re-exposure. In addition, a decrease in platelets (thrombocytopaenia) is a common observation associated with bacterial infection (Larkin *et al.*, 2016; Dewitte *et al.*, 2017), and liver function test abnormalities often accompany bacterial infections because of infection-induced haemolysis and cytokine-induced cholestasis (Minemura *et al.*, 2014). As such, systemic exposure to bacteria typically results in an immediate, profound increase in neutrophils, with possible thrombocytopaenia and hepatic abnormalities. Over the following hours to days, the T-lymphocyte response becomes evident, and

eventually, B-lymphocyte expansion and activity result in increased immunoglobulin levels.

The clinical, cellular and molecular responses seen in this study upon LPS injection into rats were consistent with the expected sequence of events for a Gram-negative bacterial infection, with the exception of a less profound lymphocyte expansion than anticipated (Alberts *et al.*, 2002). Given the severe clinical appearance and other blood metrics of inflammation seen in these rats, we believe that the flow cytometric findings should not be taken to indicate a lack of immune activation. Rather, our findings are consistent with those reported by Barnett-Vanes and colleagues in their use of LPS for pulmonary inflammation, in which they found that despite neutrophilia, LPS by itself (i.e. separate from a live bacterium) did not cause significant T-, B- or NK-cell responses in rats (Barnett-Vanes *et al.*, 2016).

In contrast to the distress caused by LPS, the injection of *S. elongatus* did not produce the response one would expect following bacterial infection. Of note, while the thrombocytopaenia seen in *S. elongatus* rats was statistically significant, it was a mild deviation which resolved within a day and was therefore likely clinically insignificant. The cytokine response of TNF-α elevation observed after *S. elongatus* injection was not statistically significant but nevertheless noteworthy. This cytokine typically increases in the setting of inflammation and is crucial for neutrophil migration and adhesion (Silveira *et al.*, 2018). Its increase 4 h following *S. elongatus* injection preceded the increase in neutrophils seen 48 h after injection in these rats. Instead of indicating acute, severe inflammation as its extraordinarily elevated levels suggested in the LPS rats, the elevation of TNF-α in *S. elongatus* rats was more likely connected with the mild, delayed neutrophilia that occurred. Separately, the increase in IgM immunoglobulins that were observed in *S. elongatus* rats was unanticipated given the lack of significant B-cell proliferation. While IgM is a well-known marker for acute infection, it is notorious for being falsely positive and should only be considered indicative of infection in the presence of other positive results (Landry, 2016). Altogether, these findings indicate that our intravenous administration of a high concentration of *S. elongatus* into rats succeeded and that the rat immune system likely was stimulated in a tempered fashion consistent with the introduction of any foreign material to the body. Importantly, *S. elongatus* was not meaningfully immunogenic and did not cause clinically significant disease.

Cyanobacteria have a modified form of LPS that is structurally distinct from common LPS and is known to be less toxic (Durai *et al.*, 2015; Simkovsky *et al.*, 2016). The LPS of *Synechococcus* strains lacks the typical inner region heptose and keto-deoxyoctulosonate (KDO) sugars, and its Lipid A portion lacks phosphates, has a single galacturonic acid and contains odd-chain hydroxylated fatty acids (Durai *et al.*, 2015). Variations in the Lipid A portion of LPS have been noted in other bacteria too, such as *C. trachomatis*, *Rhodobacter sphaeroides* and *L. pneumophila*, and are thought to be responsible for these organisms' lack of endotoxicity (Alexander and Rietschel, 2001). The specifics of the LPS structure in *S. elongatus* represents an area of ongoing research (Simkovksy *et al.*, 2016). We suspect that the lack of immune activation observed in this study may be due to this altered form of LPS that exists on the surface of *S. elongatus*.

Limitations of this study included small group sizes, particularly for the LPS positive control group; possible skewing of blood cell count data due to the substantial blood loss from repeated sampling; and the absence of a positive control for adaptive immunity. The small size of the positive control group allowed for minimization of animal distress and harm, and despite the overall small group sizes, the majority of results were highly consistent between animals. Moreover, the effect size of a clinically meaningful immunologic response was clearly evident from the observations of the LPS group. While care was taken to avoid excess blood loss during retro-orbital bleeding, the frequency of sampling resulted in reduced absolute blood cell counts. To ensure appropriate representation of results, blood cell subpopulations were reported as percentages of parent lineages or groups, instead of as absolute cell counts. Finally, a positive control was not used for the adaptive immunity portion of this study because the severe distress observed in rats that received LPS justified euthanasia before the repeat injections were to be administered. The benefit of having a positive control surrounding the repeat injections would have been to validate methodology, but in this study, the methodology from the first phase of the experiment was exactly retained in the second phase – with the exception of immunoglobulin analysis – to reduce risk of gathering misleading results.

Overall, our findings support the conclusion that *S. elongatus* is safe and non-immunogenic when administered systemically *in vivo* in rats. These results will facilitate continued research and development of cyanobacteria-related symbiotic therapies for treating tissue hypoxia.

Experimental procedures

Experimental design

The objective of this study is to characterize the clinical and biochemical response of rats to systemic administration of the cyanobacterium *S. elongatus*. To assess the acute response to this organism, male Wistar rats

(*n* = 12) were intravenously injected with *S. elongatus* and immunologic response was assessed at various time points over the subsequent 4 weeks. Two additional groups of rats were included in this study as positive and negative controls. The positive control animals (*n* = 4) received LPS from *E. coli* and the negative control animals (*n* = 12) received sterile saline (Fig. 1). After 4 weeks, a subset of the animals that received *S. elongatus* (*n* = 8) or saline (*n* = 8) received a second identical injection to investigate the adaptive immune response and were similarly monitored over the following 4 weeks. The rats' responses were characterized using clinical assessments of temperature, weight changes and signs of distress; detailed blood cell subtype quantification using complete blood counts and flow cytometric analysis; proinflammatory cytokine profiling; immunoglobulin quantification; and liver function tests. The ability of *S. elongatus* to persist in the rats was assessed by serial blood cultures and examination of all major tissues at the conclusion of the assessment period.

Propagation of S. elongatus

Synechococcus elongatus PCC 7942, previously known as *Anacystis nidulans* R2, is a unicellular, photoautotrophic, rod-shaped freshwater cyanobacterium that was originally isolated in California and has been studied internationally since the 1970s (Golden, 2019). Its genome is approximately 2.7 Mb, and it has two endogenous plasmids, all of which have been sequenced. *S. elongatus* has 2723 genes, and every locus has been surveyed for its essentiality for the organism's survival (Rubin *et al.*, 2015). *S. elongatus* was also the first cyanobacterium to be reliably transformable by exogenously added DNA (Shestakov and Khyen, 1970), and the ease of its genetic manipulation has made it popular in biotechnology research. In the context of ischaemic heart disease, *S. elongatus* may exist symbiotically with oxygen-deprived tissue by utilizing the carbon dioxide and water in mammalian tissue to produce oxygen and glucose in the presence of light. In this way, the cyanobacterium can make use of mammalian metabolic waste products and supply critical oxygen needed for the mammalian cells' continued viability. The well-studied methods of genetic modification of this organism make it particularly attractive, given the opportunities for enhancement in the context of mammalian medicine.

A slant of *S. elongatus* PCC 7942 cyanobacteria was purchased from the Pasteur Institute's Collection of Cyanobacteria (Institut Pasteur, 2019, Paris, France). The purity and genome of the bacterial sample were verified by the Pasteur Institute immediately prior to shipment of the slant. The cyanobacteria were removed from the slant and aliquoted into 25-ml sterile glass Erlenmeyer flasks with 5 ml of BG11 media each. Once these aliquots were grown into an opaque dark green solution, they were frozen into aliquots with BG11 and 5% v/v of DMSO. These were stored in cryovials at $-80\ ^{\circ}$C until use.

Approximately two weeks in advance of experiments, the frozen cyanobacteria cryovials were thawed rapidly in 37 $^{\circ}$C according to the protocol recommended by the Pasteur Institute. The cyanobacteria were then immediately centrifuged at 3000 *g* for 5 min, resuspended in fresh BG11 and grown in the dark for 3 days before being exposed to light. The cyanobacteria were maintained in glass Erlenmeyer flasks in a rotating incubator (Model no. 420, Thermo Electron Corporation, Waltham, MA, USA) under two 15 W aquarium fluorescent bulbs (Part Number 22920, General Electric, Boston, MA, USA) at 34 $^{\circ}$C and 125 rpm until used in experiments. Saturated cultures were diluted with fresh BG11 media. Throughout the study, additional purity checks were performed either by ensuring no growth when the liquid cultures were plated on Luria broth agar, or by ensuring no heterogeneous bacterial subpopulations by microscopy.

Animal care

All experiments pertaining to this investigation conformed to the Guide for the Care and Use of Laboratory Animals, published by the U.S. National Institutes of Health (Eighth Edition, 2011), under a protocol supervised by the Stanford Administrative Panel on Laboratory Animal Care, Stanford's Institutional Animal Care and Use Committee, which is accredited by the Association for the Assessment and Accreditation of Laboratory Animal Care.

Injection of rats with saline, S. elongatus and LPS

Healthy male Wistar rats (550 $\pm$ 100 g, *n* = 28) from Charles River Laboratories (Wilmington, MA, USA) were sedated in a chamber with 3.0% isoflurane (Fluriso, VetOne, Boise, ID, USA) and mechanically ventilated (Hallowell EMC, Pittsfield, MA, USA) on 2.0% isoflurane maintenance. Tail veins were dilated using a warm compress and cleaned with alcohol. Syringes containing either 1 ml of sterile saline, 2.5×10^8 cells of *S. elongatus* or LPS (150 μg kg^{-1}, from *E. coli* O111:B4, Sigma-Aldrich, St. Louis, MO, USA) were prepared in sterile conditions. To prepare the *S. elongatus* injections, the optical density was measured at 750 nm and cell concentration per mL was calculated. The appropriate volume of *S. elongatus* was centrifuged at 3000 *g* for 15 min, resuspended in 1 ml of sterile saline and transferred to a 1-ml syringe. Tail vein injections of saline

($n = 12$), *S. elongatus* ($n = 12$) or LPS ($n = 4$) were performed under sterile conditions, and the rats were recovered. Four weeks later, a second identical injection was administered to a subset of the saline ($n = 8$) and *S. elongatus* ($n = 8$) rats to specifically investigate the adaptive immune response. Injection of saline versus *S. elongatus* was randomized and all investigators except the veterinarian who administered the injections remained blinded to the group assignment until after the rats underwent necropsy and the data had been processed. Administration of LPS was not blinded given the weight-based nature of these injections and the need for additional monitoring and timely sacrifice of these animals due to severe immunologic reactions.

Blood collection and processing

Rats were sedated in a 3.0% isoflurane chamber and blood was drawn retro-orbitally immediately prior to each injection of saline, *S. elongatus* or LPS, and 4 h, 24 h, 48 h, 8 days and 4 weeks after each injection (Diehl *et al.*, 2001). Blood was collected into (i) dipotassium EDTA-coated BD Microcontainer tubes for complete blood counts (CBCs), flow cytometric analysis, and plasma preparation; (ii) sterile Eppendorf tubes for liver enzyme analysis; and (iii) vials containing 5 ml of sterile BG11 media for cyanobacteria-specific blood cultures. For CBCs, 150 μl of blood was aliquoted from the EDTA tubes for analysis. For liver enzyme analysis, the whole blood was allowed to clot and was then centrifuged to obtain serum.

S. elongatus *blood cultures*

Synechococcus elongatus-specific blood cultures were collected during each blood draw for rats receiving saline or *S. elongatus*. Peripheral blood (200–250 μl) collected into vials of 5 ml BG11 was incubated in the same rotating incubator as the *S. elongatus* stocks, exposed to constant light, for 7–10 days. A positive control containing 5 ml of BG11 plus 25 μl of *S. elongatus* from the same stock as the associated injections and a negative control containing only 5 ml BG11 were included with each group of blood culture samples. Each sample was then assessed on a Leica fluorescence microscope (DMi8 Microscope, Leica Biosystems, Wetzlar, Germany) under bright field and Texas Red fluorescence, as *S. elongatus* autofluoresces under Texas Red wavelength excitation (595 nm). Additionally, 200 μl of each sample was plated on BG11 media agar (Teknova, Hollister, CA, USA) and incubated at room temperature on a light box (A3 LED Light Pad, AGPTek, Brooklyn, NY, USA) for 3 weeks. Cyanobacterial growth was assessed based on the presence or absence of bright green colonies.

Clinical assessment

A comprehensive clinical assessment was performed on each animal immediately before each blood draw. This included measurement of weight and rectal temperature, and assessment for signs of distress (Table S2; National Research Council (US) Committee on Recognition and Alleviation of Distress in Laboratory Animals, 2008). Any additional abnormalities were noted.

Flow cytometry

To quantify lymphocyte populations, flow cytometry was performed following each blood draw. Cells were prepared by transferring 150 μl of whole blood from the EDTA-coated blood collection tube into 1.5 ml of Red Blood Cell Lysis Buffer (eBioscience, San Diego, CA, USA). After 10 min at room temperature, samples were centrifuged and resuspended in Flow Cytometry Staining Buffer (R&D Systems, Minneapolis, MN, USA). Cell counts were obtained using Trypan blue stain and a haemacytometer to ensure sufficient cells were present for analysis. Cells were resuspended at a concentration of approximately 20 million cells per ml and incubated with 1.7 μl of whole rat IgG (Jackson ImmunoResearch Laboratories, West Grove, PA, USA) for 10 min on ice to block non-specific Fc receptors.

Cells were then stained with Zombie Aqua fixable viability dye (BioLegend, San Diego, CA, USA) for 30 min and for CD3 (PerCP-eFluor 710, eBioscience), CD4 (FITC, BioLegend), CD8a (PE-Cy7, eBioscience), CD25 (BV786, BD Bioscience, San Jose, CA, USA), CD45RA (PE, BioLegend) and CD161 (APC, BioLegend) membrane proteins for 30 min (Barnett-Vanes *et al.*, 2016). They were then fixed in 4% paraformaldehyde for 10 min and resuspended in 200 μl of staining buffer for analysis. UltraComp eBeads (Invitrogen, Carlsbad, CA, USA) were used to create a compensation control for each antibody, except for the Zombie Aqua compensation control, which was created with a mixture of live cells and cells heat killed at 63 °C for 3 min. A CD25 fluorescence-minus-one (FMO) control was utilized to assist with gating (Fig. 2A–I). All samples were analysed on the 'Abbott' BD Biosciences LSR II at the Stanford Shared FACS Facility, and data were processed using FlowJo software (BD Life Sciences, Ashland, OR, USA).

Immunologic assays

Uncoated rat IgG (Catalog Number 88-50490-22, Invitrogen) and IgM (Catalog Number 88-50540-22, Invitrogen) ELISA kits were used to quantify IgG and IgM concentrations according to manufacturer instructions, using plasma that had been stored at −80 °C. Concentrations were

determined from absorbance data by parametric interpolation using GraphPad Prism 8 software. Assessment of IL-1β, IL-6, TNF-α and KC/GRO was performed using VPLEX Proinflammatory Rat Panel 2 kits (Catalog Number K15059D-2, Meso Scale Diagnostics, Rockville, MD, USA) according to manufacturer instructions and was analysed using Discovery Workbench 4.0 (Meso Scale Diagnostics). All assays were performed in duplicate.

Hepatotoxicity

Evidence of liver damage was assessed by serum liver enzyme quantification, performed at the Veterinary Diagnostic Center. Aspartate transaminase (AST), alanine transaminase (ALT), alkaline phosphatase and bilirubin were examined for all rats at baseline, 24 h after the first injection and upon necropsy.

Tissue analysis

All animals underwent necropsy at the Stanford Veterinary Diagnostic Center (SVDC) at 4 weeks after the final injection, except rats that received LPS, which underwent necropsy 8 days after injection. Tissue from all major organs was examined by a veterinary pathologist from the SVDC for abscess, injury and evidence of bacterial infection. The pathologist was blinded to the experimental groups at all times. The tissues examined included the heart, lung, liver, spleen, kidney, adrenal gland, eyes, testes, accessory sex glands, salivary gland, pancreas, lymph node, tongue, trachea, thyroid gland, thymus, oesophagus, stomach, small intestine, large intestine, skin, cerebrum, cerebellum white and brown adipose tissue and skull.

Statistical analysis

For all analyses except that of proinflammatory cytokines 4 h after injection, *S. elongatus*, saline and LPS groups were compared using two-way repeated measures ANOVA with the Geisser–Greenhouse correction for unequal variability of group differences. *Post hoc* comparisons were performed using Dunnett's tests when three groups were present surrounding the first injection (using saline as the control), and using the Sidak method when only two groups were present surrounding the second injection. For the analysis of proinflammatory cytokines at a single time point, two-tailed Student's *t*-tests were used. Adjusted *P* values are reported, and *P* values of < 0.05 were considered statistically significant. Statistical analysis was performed with GraphPad Prism 8 software (San Diego, CA, USA). Results are reported and displayed as mean $\pm$ SEM, and unless otherwise noted, *P* values compared with saline controls.

Conflict of interest

A patent related to the techniques reported in this article has been filed. J.E.C. and Y.J.W. are authors on a U.S. patent application related to this work filed by Stanford (15/136,612; filed 22 April 2016). The other authors declare that they have no competing interests.

Author contributions

K.M.W. conceptualized and designed the study, performed the experiments, analysed the data and wrote the manuscript. H.W. conceptualized and designed the study, provided training to perform experimental techniques, assisted with data interpretation and assisted with manuscript writing. M.J.P. assisted with study conceptualization and design. A.D.T. performed flow cytometry staining and data collection. M.R. assisted with flow cytometry data collection and data analysis. H.J.L. assisted with animal management, experimental material selection and preparation, and processing of blood and tissue samples. F.G. assisted with flow cytometry data collection. C.E.H. performed S. elongatus propagation and culture. A.J.C. performed S. elongatus propagation and culture and assisted with writing the manuscript. J.M.F. assisted with S. elongatus propagation and culture, and ELISA preparation. H.S.S. assisted with flow cytometry staining. K.J.J. assisted with ELISA experiments and study design. A. E. assisted with animal management and blood collection material selection and preparation. L.M.S. assisted with experimental design and method optimization. A.N.S. assisted with experimental design and method optimization. J.E.C. assisted in conceptualization and design of the study. Y.J.W. conceptualized and designed the study, and assisted in manuscript writing. All authors contributed significantly to the revision of the manuscript in preparation for publication.

References

Ades, E. (2019) *Species specific information: Rat* [WWW document]. URL http://web.jhu.edu/animalcare/procedures/rat.html.

Alberts, B., Johnson, A., Lewis, J., Raff, M., Roberts, K., and Walter, P. (2002) *Molecular Biology of the Cell. Chapter 24: The Adaptive Immune System*, 4th edn. New York, NY, USA: Garland Science.

Alexander, C., and Rietschel, E.T. (2001) Bacterial lipopolysaccharides and innate immunity. *J Endotoxin Res* 7: 167–202.

Alvarez, M., Reynaert, N., Chávez, M.N., Aedo, G., Araya, F., Hopfner, U., *et al.* (2015) Generation of viable plant-vertebrate chimeras. *PLoS ONE* 10: e0130295.

Atsumi, S., Higashide, W., and Liao, J.C. (2009) Direct photosynthetic recycling of carbon dioxide into isobutyraldehyde. *Nat Biotechnol* 27: 1177–1180.

Barnett-Vanes, A., Sharrock, A., Birrell, M.A., and Rankin, S. (2016) A single 9-colour flow cytometric method to characterise major leukocyte populations in the rat: validation in a model of LPS-induced pulmonary inflammation. *PLoS ONE* 11: e0142520.

Beutler, B. (2000) Tlr4: central component of the sole mammalian LPS sensor. *Curr Opin Immunol* 12: 20–26.

Carbonell, V., Vuorio, E., Aro, E.M., and Kallio, P. (2019) Enhanced stable production of ethylene in photosynthetic cyanobacterium *Synechococcus elongatus* PCC 7942. *World J Microbiol Biotechnol* 35: 77.

Cavendish, H. (1785) Experiments on air. *Philos Trans R Soc* 75: 372–384.

Chávez, M.N., Schenck, T.L., Hopfner, U., Centeno-Cerdas, C., Somlai-Schweiger, I., Schwarz, C., *et al.* (2016) Towards autotrophic tissue engineering: photosynthetic gene therapy for regeneration. *Biomaterials* 75: 2–36.

Codd, G.A., Morrison, L.S., and Metcalf, J.S. (2005) Cyanobacterial toxins: risk management for health protection. *Toxicol Appl Pharmacol* 203: 264–272.

Cohen, J.E., Goldstone, A.B., Paulsen, M.J., Shudo, Y., Steele, A.N., Edwards, B.B., *et al.* (2017) An innovative biologic system for photon-powered myocardium in the ischemic heart. *Sci Adv* 3: e1603078.

Darby, I.A., and Hewitson, T.D. (2016) Hypoxia in tissue repair and fibrosis. *Cell Tissue Res* 365: 553–562.

Dewitte, A., Lepreux, S., Villeneuve, J., Rigothier, C., Combe, C., Ouattara, A., and Ripoche, J. (2017) Blood platelets and sepsis pathophysiology: a new therapeutic prospect in critically ill patients? *Ann Intens Care* 7: 115–133.

Diehl, K.H., Hull, R., Morton, D., Pfister, R., Rabemampianina, Y., Smith, D., *et al.* (2001) A good practice guide to the administration of substances and removal of blood, including routes and volumes. *J Appl Toxicol* 21: 15–23.

Durai, P., Batool, M., and Choi, S. (2015) Structure and effects of cyanobacterial lipopolysaccharides. *Mar Drugs* 13: 4217–4230.

Fleming, K.E., and O'Shea, E.K. (2018) An RpaA-dependent sigma factor cascade sets the timing of circadian transcriptional rhythms in *Synechococcus elongatus*. *Cell Rep* 25: 2937–2945.

Gholipourmalekabadi, M., Zhao, S., Harrison, B.S., Mozafari, M., and Seifalian, A.M. (2016) Oxygen-generating biomaterials: a new, viable paradigm for tissue engineering? *Trends Biotechnol* 34: 1010–1021.

Golden, S.S. (2019) The international journeys and aliases of *Synechococcus elongatus*. *NZ J Bot* 57: 70–75.

Hamilton, T.L., Bryant, D.A., and Macalady, J.L. (2016) The role of biology in planetary evolution: cyanobacterial primary production in low-oxygen Proterozoic oceans. *Environ Microbiol* 18: 325–340.

Heesterbeek, D.A.C., Angelier, M.L., Harrison, R.A., and Rooijakkers, S.H.M. (2018) Complement and bacterial infections: from molecular mechanisms to therapeutic applications. *J Innate Immun* 10: 455–464.

Heumann, D., and Roger, T. (2002) Initial responses to endotoxins and gram-negative bacteria. *Clinica Chemica Acta* 323: 59–72.

Jochimsen, E.M., Carmichael, W.W., An, J.S., Cardo, D.M., Cookson, S.T., Holmes, C.E., *et al.* (1998) Liver failure and death after exposure to microcystins at a hemodialysis center in Brazil. *N Eng J Med* 338: 873–878.

Karim, M.Y., and Fadi, G.L. (2015) A brief journey through the immune system. *Clin J Am Soc Nephrol* 10: 1274–1281.

Kaya, Z., Tretter, T., Schlichting, J., Leuschner, F., Afanasyeva, M., Katus, H.A., and Rose, N.R. (2005) Complement receptors regulate lipopolysaccharide-induced T-cell stimulation. *Immunology* 114: 493–498.

Landry, M.L. (2016) Immunoglobulin M for acute infection: true or false? *Clin Vaccine Immunol* 23: 540–545.

Larkin, C.M., Santos-Martinez, M.J., Ryan, T., and Radomski, M.W. (2016) Sepsis-associated thrombocytopenia. *Thromb Res* 141: 11–16.

Martin, I., Cabán-Hernández, K., Figueroa-Santiago, O., and Espono, A.M. (2015) Fasciola hepatica fatty acid binding protein inhibits TLR4 activation and suppresses the inflammatory cytokines induced by lipopolysaccharide in vitro and in vivo. *J Immunol* 194: 3924–3936.

Minemura, M., Tajiri, K., and Shimizu, Y. (2014) Liver involvement in systemic infection. *World J Hepatol* 6: 632–642.

National Research Council (US) Committee on Recognition and Alleviation of Distress in Laboratory Animals. (2008) *Recognition and Alleviation of Distress in Laboratory Animals. Recognition and Assessment of Stress and Distress*. Washington, DC, USA: National Academies Press (US), 3.

Institut Pasteur. (2019) *The Pasteur Culture Collection of Cyanobacteria (PCC)* [WWW document]. URL https://www.pasteur.fr/en/public-health/crbip/distribution/pcc.

Rubin, B.E., Wetmore, K.M., Price, M.N., Diamond, S., Shultzaberger, R.K., Lowe, L.C., *et al.* (2015) The essential gene set of a photosynthetic organism. *Proc Natl Acad Sci USA* 112: E6634–E6643.

Santos-Merino, M., Garcillán-Barcia, M.P., and de la Cruz, F. (2018) Engineering the fatty acid synthesis pathway in *Synechococcus elongatus* PCC 7942 improves omega-3 fatty acid production. *Biotechnol Biofuels* 11: 239.

Shestakov, S.V., and Khyen, N.T. (1970) Evidence for genetic transformation in blue-green alga *Anacystis nidulans* R2. *Molec Gen Genet* 107: 372–375.

Silveira, A.A., Dominical, V.M., Almeida, C.B., Chiweih, H., Ferreira, W.A. Jr, Vicente, C.P., *et al.* (2018) TNF induces neutrophil adhesion via formin-dependent cytoskeletal reorganization and formation of β-integrin function. *J Leukoc Biol* **103:** 87–98.

Simkovsky, R., Effner, E.E., Iglesias-Sánchez, M.J., and Golden, S.S. (2016) Mutations in novel lipopolysaccharide biogenesis genes confer resistance to amoebal grazing in *Synechococcus elongatus. Appl Environ Microbiol* **82:** 2738–2750.

Stewart, I., Webb, P.M., Schluter, P.J., and Shaw, G.R. (2006) Recreational and occupational field exposure to freshwater cyanobacteria – a review of anecdotal and case reports, epidemiological studies and the challenges for epidemiologic assessment. *Environ Health* **5:** 6.

Wang, H., Wu, M.A., and Woo, Y.J. (2019) Photosynthetic symbiotic therapy. *Aging* **11:** 843–844.

Supporting information

Additional supporting information may be found online in the Supporting Information section at the end of the article.

Fig S1. Temperature and weight changes over time. Clinical characteristics that were assessed immediately before each blood draw for rats injected with saline (n = 8-12), *S. elongatus* (n = 8–12), or LPS (n = 4). Those injected with LPS became febrile and lost weight while those injected with saline or *S. elongatus* did not. Error bars represent SEM, black arrows indicate time of injection. d: days. h: hours. LPS: Lipopolysaccharide. w: weeks. *=significant vs. saline ($P < 0.05$), ***=significant vs. saline ($P = 0.0001$).

Fig S2. White blood cell (WBC) and platelet changes over time. Findings from CBC analysis of rats injected with saline (n = 8–12), *S. elongatus* (n = 8–12), or LPS (n = 4), demonstrating comparable values for rats that received saline or *S. elongatus*, and marked thrombocytopenia and leukopenia in those that received LPS. Error bars represent

SEM, and black arrows indicate time of injection. d: days. h: hours. LPS: Lipopolysaccharide. w: weeks. *=significant vs. saline ($P < 0.05$), **=significant vs. saline ($P < 0.01$), ***=significant vs. saline ($P < 0.001$), ****=significant vs. saline ($P < 0.0001$).

Fig S3. White blood cell (WBC) differentials by group. WBC differentials for rats injected with saline (n = 8–12), *S. elongatus* (n = 8–12), or LPS (n = 4), indicate a neutrophil shift after injection for all groups, but most quickly and profoundly in rats that received LPS. Black arrows indicate time of injection. d: days. h: hours. LPS: Lipopolysaccharide. w: weeks. *=significant vs. saline ($P < 0.05$), **=significant vs. saline ($P < 0.01$), ***=significant vs. saline ($P < 0.001$), ****=significant vs. saline ($P < 0.0001$).

Fig S4. Absolute numbers of white blood cell subtypes. Absolute white blood cell counts from complete blood counts (CBCs) of rats injected with saline (n = 8–12), *S. elongatus* (n = 8–12), or LPS (n = 4), demonstrating comparable responses for rats that received saline or *S. elongatus*, and neutrophilia and complementary lymphopaenia in rats that received LPS. Error bars represent SEM, and black arrows indicate time of injection. d: days. h: hours. LPS: Lipopolysaccharide. w: weeks. *=significant vs. saline ($P < 0.05$), **=significant vs. saline ($P < 0.01$), ***=significant vs. saline ($P < 0.001$), ****=significant vs. saline ($P < 0.0001$).

Table S1. Liver function test results from 24 h after the first injection. Values of liver enzymes and bilirubin 24 h after the first injection displayed mild liver enzyme elevations in LPS rats, relative to saline controls. IU: International units. LPS: Lipopolysaccharide. U: Enzyme units. *=significant vs. saline ($P < 0.05$), **=significant vs. saline ($P < 0.01$), ***=significant vs. saline ($P < 0.001$), ****=significant vs. saline ($P < 0.0001$).

Table S2. Signs of distress that were evaluated during clinical assessment. This list of signs of distress in rats was adapted from the National Research Council Committee on Recognition and Alleviation of Distress in Laboratory Animals (34). Each rat was examined prior to every blood draw during the study, and these signs were specifically assessed. Other abnormalities were also noted.